Spatial variation of pure and simple shear across transpressive shear zones: flow kinematics map of the Posada-Asinara shear zone (NE Sardinia, Italy)

Alessandro Petroccia[1]

[1] Department of Earth Sciences, University of Turin, Via Valperga Caluso 35, 10125, Torino, Italy.

AP, 0000-0001-5230-0046.

Rend. Online Soc. Geol. It., Vol. 60 (2023), pp. 24-36, 5 figs., 1 tab., https://doi.org/10.3301/ROL.2023.28

Article

Corresponding author e-mail: alessandrogiovannimichele.petroccia@unito.it

Citation: Petroccia A. (2023) - Spatial variation of pure and simple shear across transpressive shear zones: flow kinematics map of the Posada-Asinara shear zone (NE Sardinia, Italy). Rend. Online Soc. Geol. It., 60, 24-36, https://doi.org/10.3301/ROL.2023.28.

Associate Editor: Gianluca Vignaroli

Submitted: 21 November 2022

Accepted: 24 February 2023

Published online: 18 April 2023

SOCIETÀ GEOLOGICA ITALIANA
FONDATA NEL 1881 · ENTE MORALE R. D. 17 OTTOBRE 1885

ABSTRACT

Flow kinematics estimations are necessary to determine how the deformation is partitioned in shear zones at different scales. Combining different scales of structural analysis with quantitative vorticity constraint allows a more rigorous examination of the kinematics of deformation. The Posada-Asinara shear zone (PASZ) in northern Sardinia (Italy) is a crustal-scale km-thick transpressive shear zone, separating the High- from the Medium-Grade Metamorphic Complex. After microstructural analysis, the vorticity of the flow was estimated to investigate the southernmost boundary of the PASZ, highlighting a dominant pure shear component far from the core of the shear zone. These results have been integrated with existing data to derive a regional-scale flow kinematic map of the Baronie region, highlighting the potentiality of automated geostatistical mapping to become a powerful complementary tool in the investigation of flow kinematics in collisional environments.

KEY-WORDS: Variscan belt, transpression, vorticity, mylonite, strain partitioning.

INTRODUCTION

Understanding how the lithosphere accommodates continental collision at plate boundaries remains an important issue in tectonics for both recent and old orogenic belts (e.g., Conand et al., 2020; Torvela & Kurhila, 2020). In an oblique collisional setting, deformation can be partitioned by combining lateral horizontal flow (i.e., escape), thrusting along the direction of shortening (Cagnard et al., 2006; Chardon et al., 2009; Bajolet et al., 2015) or coeval development of thrust, strike-slip, and mixed zones through orogens (Teyssier & Whitney, 2002; Iacopini et al., 2008; Nabavi et al., 2017, 2020). All tectonic regimes are significantly enhanced in the context of orocline formation (Bajolet et al., 2013; Johnston et al., 2013; Krýza et al., 2019; Parui et al., 2022). Transpression, involving both strike-slip and contractional deformation, has been conceptually introduced to explain structures within oblique convergent plate boundaries during the collision (e.g., Harland, 1971; Sanderson & Marchini, 1984; Tikoff & Fossen, 1993; Teyssier et al., 1995; Sullivan & Law, 2007; Sarkarinejad & Azizi, 2008), playing a relevant role during the exhumation of high-grade metamorphic rocks (Dewey et al., 1998; Jones et al., 2004; Dasgupta et al., 2015).

Field-based studies are still necessary when exploring any type of shear zones (e.g., Montomoli et al., 2013; Carosi et al., 2016; Caso et al., 2021; Oberto & Petroccia, 2021; Ortolano et al., 2022; Petroccia et al., 2022b), but a quantitative assessment of the flow kinematic is required (e.g., Simpson & De Paor, 1993; Xypolias, 2010). In fact, contrary to the first proposed models, where the deformation in shear zones has been related only to simple shear, it is now widely accepted that high-strain zones evolve through the combination of simple and pure shear components (see Xypolias, 2010 and Fossen & Cavalcante, 2017 for a review). Also, different amounts of pure and simple shear relative to the structural distance from the shear zone are often recognizable (Fossen & Cavalcante, 2017; Nania et al., 2022; Petroccia et al., 2022a). Therefore, the quantitative estimation of flow kinematics in sheared rocks is necessary for investigating the nature and spatial distribution of the deformation within shear zones (e.g., Law et al., 2004; Carosi et al.,

2006; Xypolias & Kokkalas, 2006; Forte & Bailey, 2007; Thigpen et al., 2010; Ring et al., 2015; Nabavi et al., 2017; Montemagni et al., 2020; Ortolano et al., 2020; Simonetti et al., 2021; Ghosh & Bhattacharyya, 2022; Montemagni & Zanchetta, 2022).

The degree of non-coaxial deformation and the partitioning between pure and simple shear can be constrained by determining the kinematic vorticity parameter (W_k; Xypolias, 2010). Although contour maps are widely used in Earth Sciences to show the variation of quantities over the surface (Groshong, 2006), relatively few attempts have been made to exploit the potential usefulness of these maps in flow kinematic analysis (e.g., Sarkarinejad & Heibati, 2017). A graphical representation of the flow kinematic distribution at the map scale could be a helpful tool for investigating the W_k spatial variation of shear zones, identifying zones affected by different amounts of simple and pure shear.

The evolution of the Variscan chain in Europe is characterized by the development of crustal-scale strike-slip shear zones during the Late Carboniferous (Arthaud & Matte, 1977; Matte, 2001; Carreras & Druguet, 2014; Franke et al., 2017; Cochelin et al., 2021; Faure & Ferrière, 2022). In particular, the southern European Variscan belt was widely affected by the development of a network of crustal-scale dextral transpressive shear zones called the East Variscan Shear Zone (EVSZ; Corsini & Rolland, 2009; Carosi et al., 2012; Padovano et al., 2012, 2014; Simonetti, 2021). Its activity is now well-constrained in different parts of its branches and is related to Carboniferous transpression (see Carosi et al., 2022 for a review). Various multidisciplinary studies have provided detailed structural, kinematic, and petrochronological investigations in different portions of the Variscan belt affected by the EVSZ, i.e., the Aiguilles-Rouges, Aar-Gotthard Massif and Mont-Blanc Massif (Von Raumer & Bussy, 2004; Simonetti et al., 2020a; Bühler et al., 2022; Vanardois et al., 2022), the Belledonne-Pelvoux Massifs (Freville et al., 2022), the Argentera Massif (Simonetti et al., 2018, 2021), the Maures-Tanneron Massif (Schneider et al., 2014; Simonetti et al., 2020b; Simonetti, 2022), and Corsica-Sardinia block (Carosi & Oggiano, 2002; Carosi & Palmeri, 2002; Giacomini et al., 2008; Faure et al., 2014; Carosi et al., 2020). All these transpressional shear zones are characterized by a significant amount of pure shear acting alongside simple shear, confirming their important role during the exhumation of the internal zones from the early stages of transpression until later gravitational collapse. Thus, the Variscan chain in Sardinia represents an excellent example where it is possible to explore the tectonic mechanisms affecting the crust during the evolution from perpendicular collision to orogen-parallel transpression in the context of an oblique collision (Carosi & Palmeri, 2002).

In this work, a sector of the Posada-Asinara shear zone (PASZ; Carosi & Palmeri, 2002) located in the NE Sardinia (Baronie region) has been investigated (Fig. 1). Although multidisciplinary studies are already available (Carosi et al., 2020 and reference therein), no kinematic constraints about the most external boundary of the PASZ are present. This paper aims to fill the gap concerning the lack of kinematic data in the southernmost sector of the PASZ. An updated complete regional-scale kinematic vorticity distribution map of the PASZ in the Baronie region (NE Sardinia) has been provided by combining the newly collected data with the existing dataset.

GEOLOGICAL SETTING

The shape of the Variscan belt in Europe results from a Devonian-Carboniferous continent-continent collision between Laurentia-Baltica and Gondwana (Matte, 1986, 2001). The metamorphic basement of the Sardinia island represents a fragment of the southern European Variscan belt and, due to the lack of the Alpine overprint, it represents a good locality to investigate the Paleozoic tectono-metamorphic evolution (Carmignani et al., 1994; see Cruciani et al., 2015 for a critical review). The Sardinian Variscan belt is characterized by a northward increase in metamorphic grade from the External Zone or the foreland (SW) to the Inner Zone or the hinterland (NE).

The Nappe Zone in Sardinia (i.e., the hinterland-foreland transition zone) has been divided into External (central to southern Sardinia) and Internal (northern to central Sardinia) Nappe Zone (Carmignani et al., 1994; Carosi & Pertusati, 1990; Conti et al., 1999, 2001; Casini & Oggiano, 2008; Casini et al., 2010; Cocco et al., 2018, 2022; Montomoli et al., 2018; Petroccia et al., 2022a, b, c). The boundary between them is marked by a regional-scale, top-to-the S-SW thrust-sense ductile to brittle shear zone, the Barbagia Thrust (BT; Carosi & Malfatti, 1995; Conti et al., 1998; Montomoli et al., 2018; Petroccia et al., 2022a, b). The Internal Nappe Zone comprises: (i) the Low-Grade Metamorphic Complex (LGMC; Barbagia, Goceano, and southern Nurra units; Carmignani et al., 1994; Montomoli, 2003; Casini & Oggiano, 2008), which reached greenschist-facies metamorphic conditions, and (ii) the Medium-Grade Metamorphic Complex (MGMC; Baronie, Anglona, and northern Nurra units; Carmignani et al., 1994, 2001) which reached amphibolite-facies conditions (Cruciani et al., 2015, 2022). The Axial or Inner zone, located in the northernmost sector of the Sardinia island, belongs to the High-Grade Metamorphic Complex (HGMC), mainly made by high-pressure (H*P*) migmatite, migmatized orthogneiss, calc-silicate nodule, and metabasite lense preserving eclogite and granulite-facies relics (Franceschelli et al., 2005; Massonne et al., 2013; Casini et al., 2023). The boundary zone between the L-MGMC and the HGMC is marked by the Posada-Asinara shear zone (PASZ; Elter et al., 1990; Fig. 1a), a 150 km long and 10–15 km wide dextral transpressive Late-Variscan shear zone (Carosi & Palmeri, 2002; Carosi et al., 2005, 2009, 2012; Frassi et al., 2009), recognizable along the Posada Valley and within the northern sector of the Asinara island (Carosi et al., 2004; Iacopini et al., 2008). The PASZ developed under decreasing temperature conditions, from amphibolite- to greenschist-facies (Graziani et al., 2020; Cruciani et al., 2022). The amphibolite-facies is confirmed by the syn-kinematic sillimanite + biotite or biotite + white mica parallel to the mylonitic foliation (Carosi et al., 2020). This also agrees with the occurrence of grain boundary migration (GBM) as the main dynamic recrystallization mechanism of quartz, indicative of temperatures higher than ~500 °C (Law, 2014). The presence of chlorite highlights a decrease in the metamorphic conditions, supported by incipient sub-grain rotation recrystallization (SGR) overprinting GBM in quartz (Graziani et al., 2020). The PASZ displays a strong deformation gradient and strain partitioning, with an increase of both simple shear component and strain intensity along the deformation gradient (i.e., toward the N; Carosi et al., 2020). *In-situ* Ar-Ar dating of white mica (Di Vincenzo et al., 2004) and U–(Th)–Pb dating of monazite (Carosi et al., 2012, 2020; Cruciani et al., 2022)

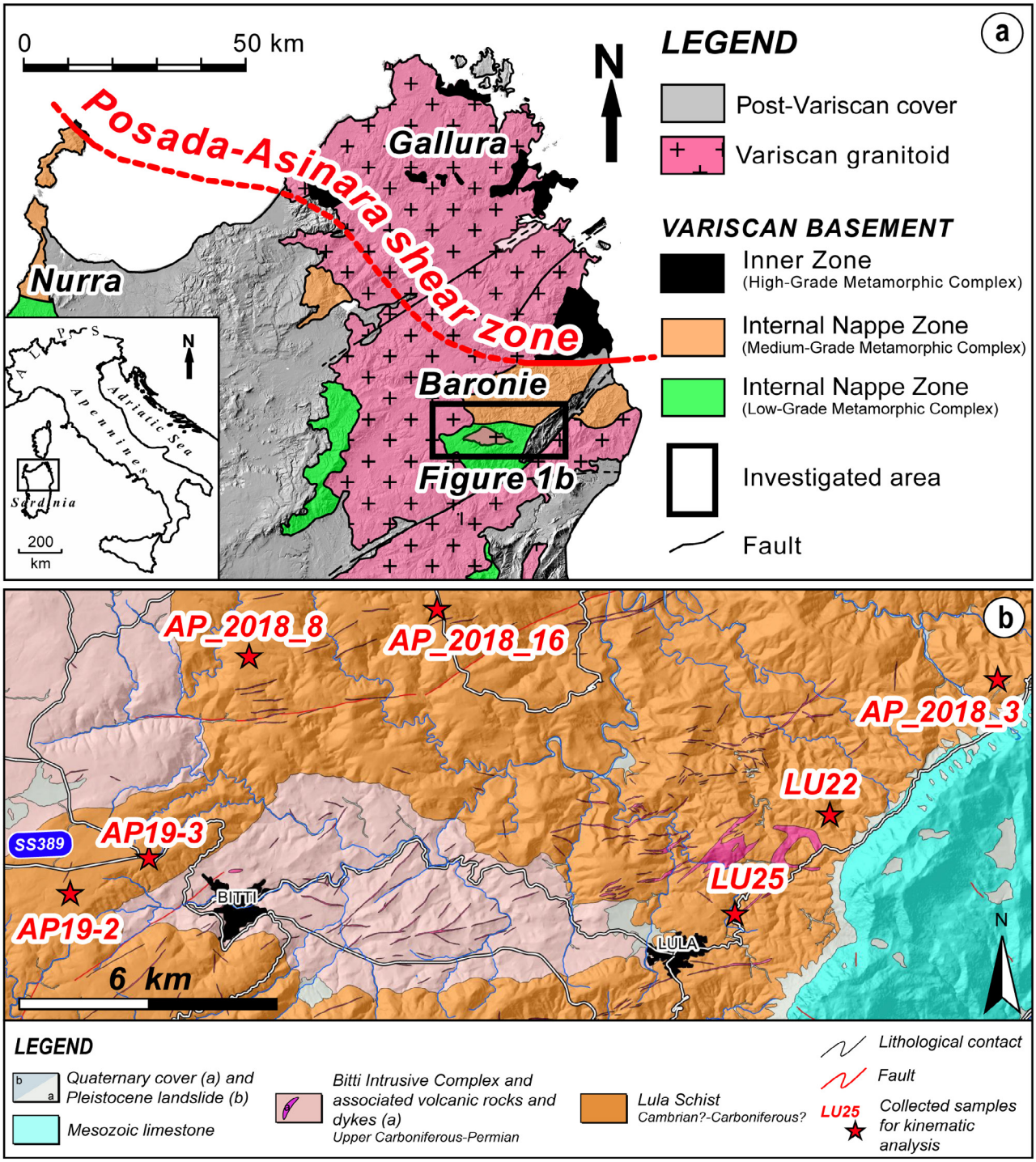

Fig. 1 - a) tectonic sketch map of northern Sardinia showing the main geological zones (modified after Carosi et al., 2020); b) simplified geological map of the studied area with the location of the analyzed samples (red stars).

constrained the age of the transpressional shear activity in a time span of 25 Ma, from 325 to 300 Ma.

A metamorphic zonation from the garnet to the sillimanite + white mica zone characterizes the Paleozoic metasedimentary sequence of the Baronie region (Franceschelli et al., 1982, 1989). The garnet zone is further subdivided into garnet + albite and garnet + oligoclase sub-zones. The investigated area in NE Sardinia (Baronie region) includes the southernmost sector deformed by the PASZ shearing, and it is located at the boundary between the L- and the MGMC (Fig. 1a), where the garnet + albite and garnet + oligoclase-bearing micaschist and paragneiss enclosed in the Lula Schist (Fig. 1b) crop out.

METHODOLOGY

A numerical progression, following Carosi et al. (2020), has been used to describe deformation phases and structural elements (e.g., S_1, S_2). Microstructural analyses were performed on field-oriented samples, cut perpendicular to the main foliation and

parallel to the object lineation (approximating the XZ section of the finite strain ellipsoid). Foliations have been classified according to Passchier & Trouw (2005). Quartz dynamic recrystallization microstructures are defined according to Stipp et al. (2002) and Law (2014). Mineral abbreviations are after Warr (2021).

Kinematics of the flow

Pure and simple shear components could be described through the dimensionless mean kinematic vorticity parameter (W_m). Since its introduction into the geological literature, vorticity analysis methodologies have become increasingly sophisticated (e.g., Tikoff & Fossen, 1995; Jessup et al., 2007; Xypolias, 2010; Fossen, 2016). The non-coaxial deformation can be normalized to the stretching along the strain axes to obtain a dimensionless number, i.e., the kinematic vorticity parameter. It could be derived through the relation proposed by Passchier (1987):

$$W_k = W/|d2 - d3|$$

where W represents the vorticity and d2−d3 represents the stretching difference along the intermediate and minimum principal strain axes. The mean kinematic vorticity number (W_m) could be assumed to be equal to W_k because it represents the average value over the deformation interval during which the structure or fabric developed (Xypolias, 2010; Fossen & Cavalcante, 2017). Pure and simple shear is associated with $W_k = 0$ and $W_k = 1$, respectively. Simple and pure shear contribute equally during the deformation when $W_k = 0.71$ (Law et al., 2004; Passchier & Trouw, 2005; Xypolias, 2010). The absolute error of vorticity results is ±0.1 (Tikoff & Fossen, 1995). However, comparing different possible systematic error sources highlights a more realistic minimum systematic error of ±0.2 (Iacopini et al., 2011).

In any type of flow, it is possible to recognize two planes representing the flow apophyses (A_1 and A_2), along which the particles do not undergo rotation. They are orthogonal in a pure shear dominated deformation and coincide with each other during a simple shear flow. The applied *C'* shear band method (Kurz & Northrup, 2008) is based on the measurement of the orientation of *C'* planes with respect to the shear zone boundaries. This approach is based on the assumption that the *C'* planes nucleated as a bisector of the angle between the two apophyses and the *C* planes are parallel to the shear zones boundaries and the A_2 apophyses, respectively. The vorticity number can be derived through the relation:

$$W_k = \cos 2v$$

where 2v represents the angle between the two flow apophyses (see Kurz & Northrup, 2008; Gillam et al., 2013 for methodological details; Fig. 2a). Due to the progressive rotation of the structural elements during the flow, including *C'* planes, it is necessary to consider the maximum v values, among those measured, as the closest approximation of the initial nucleation angle of the *C'* plane. Kurz & Northrup (2008) demonstrated that the average value of the measured v angles is not representative of the original angle of nucleation of *C'* planes. Examples of polar histograms used to derive the angle v are provided in Fig. 2b.

To establish the type of deformation, i.e., the deformation regime, the angle θ between the maximum Instantaneous Stretching Axis (ISA max) in the horizontal plane and the shear zone boundary has been calculated. This parameter is fundamental

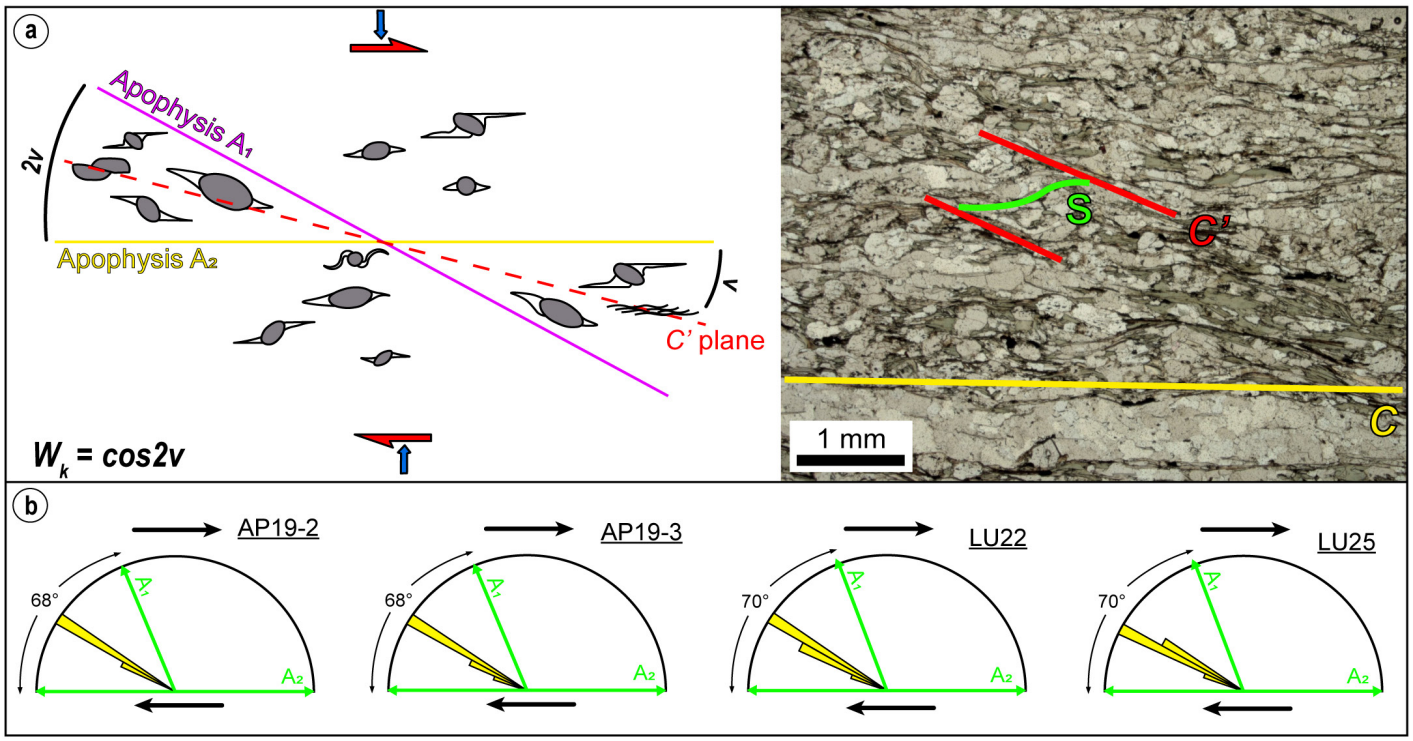

Fig. 2 - a) schematic diagram of microstructures developed under general flow conditions in a mylonite with a dextral sense of shear is displayed. The equation to calculate the W_k parameter is also shown (modified after Kurz & Northrup, 2008). In the right part, a thin section photo showing the observed and investigated mylonitic fabric is provided; b) examples of the polar histograms used for the *C'* shear band method.

for distinguishing between transpression and transtension (Fossen & Tikoff, 1993; Fossen et al., 1994). The calculation was performed using the formula proposed by Xypolias (2010):

$$\theta = (\arcsin W_k)/2$$

According to Fossen et al. (1994) θ angles larger than 45° are indicative of transtensive deformation, while θ angles smaller than 45° are indicative of transpressional deformation.

Contour map

Different types of interpolations, based on deterministic or stochastic mathematical models, exist. Deterministic interpolation (e.g., IDW, Natural Neighbour; Boissonnat & Gazais, 2002) assigns a value based on the neighbouring measured parameters and deals with systematic and univocal value distributions as opposed to random ones. Stochastic interpolators (e.g., Kriging) depend on the computation of a probability model, which is a mathematical representation of a random phenomenon. For geological data interpolation, is often difficult to acquire large amounts of homogeneously distributed data according to a regular sampling grid. It is important to note that the level of statistical reliability depends on the neighbourhood distribution and the density of the georeferenced samples.

Integrating these results with the existing vorticity data in this sector of the PASZ taken with the same *C'* shear band vorticity method (Carosi et al., 2020), a regional-scale W_k-distribution map of the Baronie area has been derived. The contouring procedure has been developed using IG-Mapper (Fiannacca et al., 2017), an ArcGIS toolbox in the ArcMap 10.8 environment that comprises sixteen tools. This procedure is based on ordinary Kriging as a stochastic interpolation method.

MICROSTRUCTURES OF THE PASZ

The D_2 structures overprint pervasively the plagioclase + garnet-bearing micaschist and paragneiss (see the geological maps in Fig. 1b). A variation in structural style moving northward across the deformation gradient occurs. The intensity of deformation increases toward the PASZ, as does the foliation becomes progressive mylonitic. Sheared metasedimentary rocks are characterized by a northward transition from a well-developed discrete, smooth and spaced foliation with zonal cleavage domains up to a continuous cleavage. In many samples, a penetrative continuous mylonitic foliation is found. It is worth noting that the frequency of the occurrence of the D_1 structures decreases approaching the PASZ, due to the D_2 overprinting and transposition.

The main foliation (S_2) is defined by the preferred orientation of mm-thick levels of white mica, biotite and minor chlorite alternated with quartz-rich layers. The S_2 foliation wraps around albite/oligoclase (Fig. 3a) and garnet porphyroclasts. A sporadic internal foliation (S_1), made of orientated quartz, white mica, ilmenite, rutile and graphite, varying from discordant to concordant with the external one, is recognizable (Fig. 3a, b). This suggests that plagioclase and garnet could be inter- to early syn-tectonic (syn-S_2) minerals with respect to the S_2 (i.e., between the D_1 and D_2 phases and during the early D_2 phase). Rarely, in the southernmost investigated samples, S_1 foliation can be identified in the hinge zone of the micro-scale F_2 folds or microlithons (Fig. 3c). Quartz in mylonite displays undulose extinction and tilt walls. Quartz lobate and ameboid grain boundaries, window and pinning structures (Fig. 3d) suggest dynamic recrystallization by GBM, indicative of T > 500 °C (Law, 2014). In some samples, quartz shows new grains of smaller size surrounding larger crystals forming a "core and mantle structure", with weakly bimodal grain size, indicating an overprinting of SGR on GBM. Kinematic indicators pointing to a top-to-the NW sense of shear, such as *C'*-*C*-S fabric (Fig. 3e), σ- and δ-type porphyroclasts (Fig. 3f), asymmetric strain fringes around porphyroclasts (Fig. 3g) and mica-fish, are present. Although chlorite generally overgrows both garnet and biotite, it is also recognizable parallel to both the main foliation and *C'* plane or defining the asymmetric strain fringes around porphyroclasts (Fig. 3g). This highlights that the PASZ activity also continued under greenschist-facies conditions. Late F_3 kink folds affecting all previous structural elements with no syn-metamorphic blastesis are recognizable (Fig. 3h).

FLOW KINEMATICS ESTIMATIONS

A total of seven samples (see Fig. 1b for sample location), including garnet- and plagioclase-bearing micaschists and paragneiss from the southern sector of the PASZ, were analyzed (Fig. 1b). Vorticity analyses were performed on sections parallel to the object lineation and perpendicular to the mylonitic foliation (XZ plane of the finite strain ellipsoid; Fig. 2a). Results of the kinematic vorticity analysis with *C'* shear band method and calculated θ angle are reported in Table 1.

Table 1 - Summary Table of the vorticity data obtained with the *C'* shear band method: number of data (N), the angle between *C'* planes and the shear zone boundary (v), vorticity value (W_k), angles between the maximum ISA in the horizontal plane and the shear zone boundary (θ).

SAMPLE NAME	N	v ANGLE (°)	2v ANGLE (°)	W_k	θ ANGLE (°)
AP19-2	41	34	68	0.37	11
AP19-3	32	33	66	0.41	12
LU22	28	33	66	0.41	12
LU25	32	32	64	0.44	13
AP_2018_8	12	33	66	0.41	12
AP_2018_16	10	31	62	0.47	14
AP_2018_3	18	31	62	0.47	14

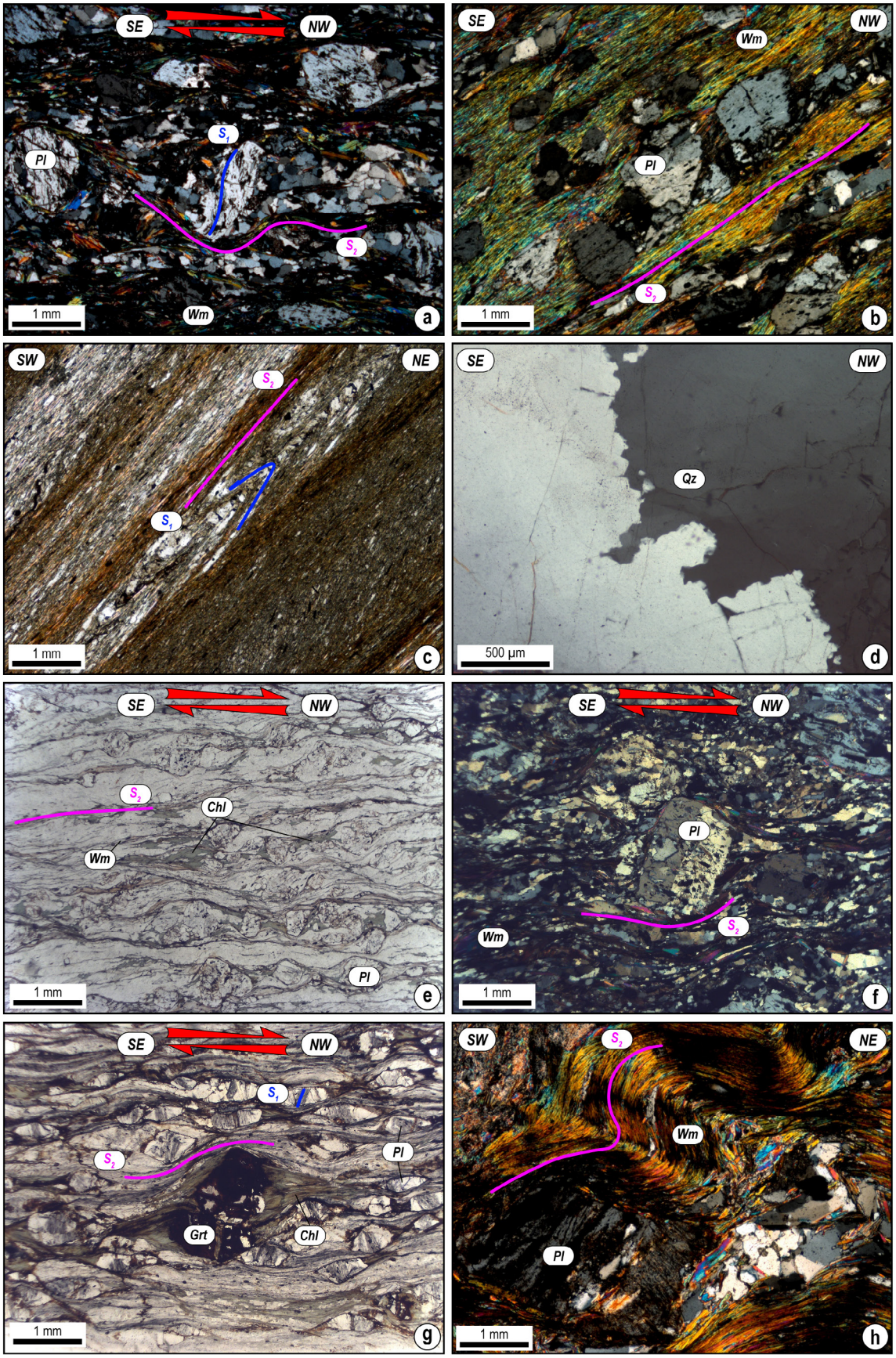

Fig. 3 - a) plagioclase porphyroclast showing an internal foliation S_1 (blue line), wrapped by the main foliation S_2 (pink line) (XPL; crossed-polarized light); b) white mica and biotite defining the S_2 and the internal foliation of a syn-D_2 plagioclase porphyroblasts (XPL); c) S_2 spaced crenulation cleavage (PPL; plane-polarized light); d) dynamically recrystallized quartz in plagioclase-bearing micaschist showing lobate and irregular grain boundaries indicative of GBM (XPL); e, f, g) different kinematic indicators (*C'*-*C*-*S* fabric and asymmetric porphyroclast or strain fringes) linked to the PASZ activity showing a top-to-the NW sense of shear; h) F_3 micro-folds affecting the S_2 foliation (XPL).

Vorticity values range between 0.47 and 0.37 (Fig. 4a), with a mean of 0.43 and a mode of 0.41. The obtained vorticity values indicate that this sector of the PASZ experienced general shear (Forte & Bailey, 2007) during deformation, which involved 75-68% pure shear and 25-32% simple shear components (Fig. 4b). These results indicate a flow regime characterized by an important contribution of pure shear. Calculated θ angles between the maximum Instantaneous Stretching Axis (ISA max) in the horizontal plane and the shear zone boundary vary between 11-14°. These values indicate a pure shear dominated transpression deformation (Fig. 4c).

Integrating these results with the existing flow kinematics data in this sector of the PASZ (Petroccia, 2018; Carosi et al., 2020), a regional-scale W_k-distribution map of the Baronie area has been derived (Fig. 5).

DEFORMATION REGIME MAP AND FINAL REMARKS

The PASZ is an orogen-parallel transpressional shear zone that drove the exhumation of the Sardinian HGMC. The evidence of D_1 structures is represented by S_1 relict foliation in the hinge of F_2

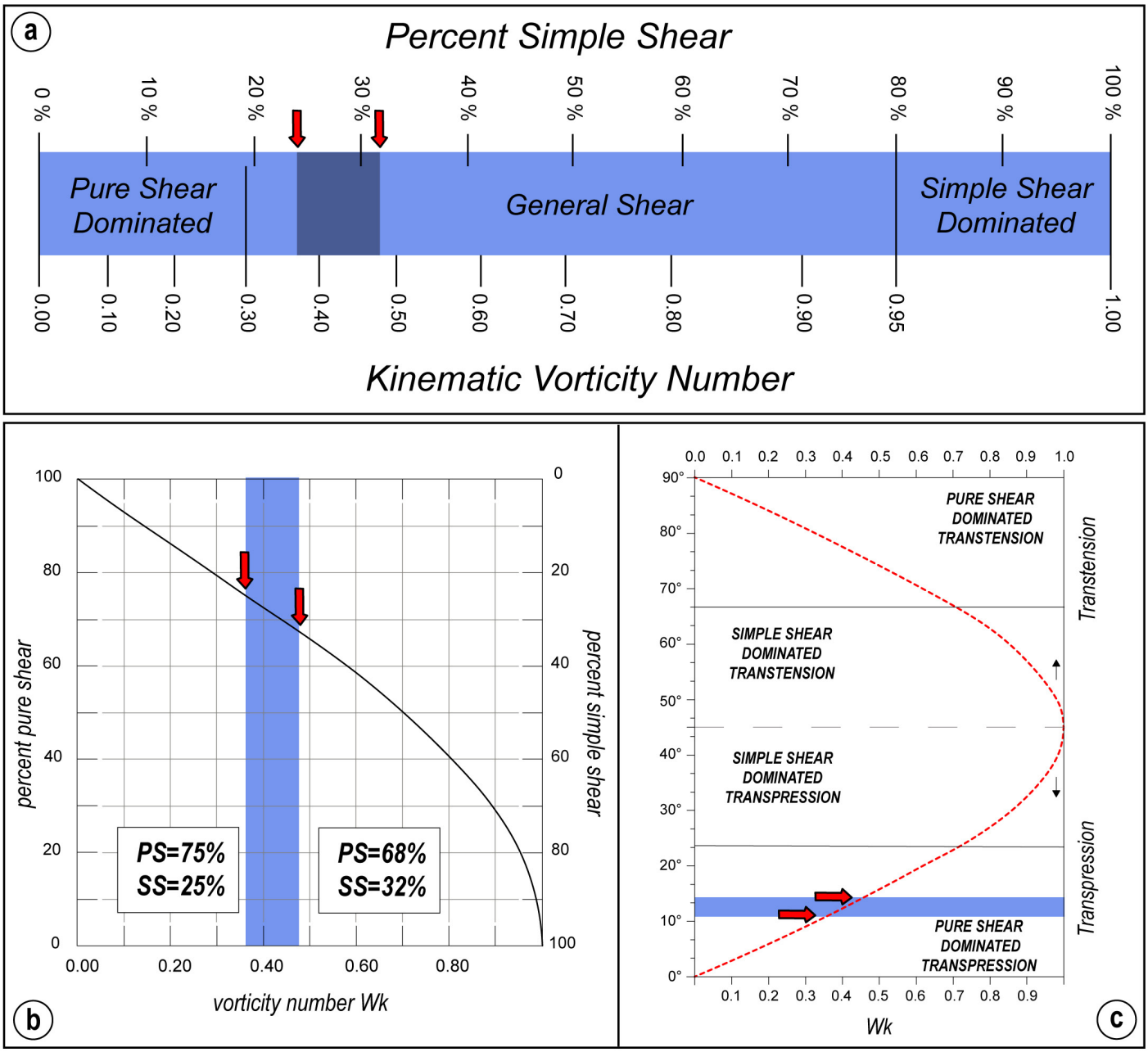

Fig. 4 - a) Relation between the kinematic vorticity number W_k and the percent of simple shear. Pure shear, general shear and simple shear dominated deformation regimes are marked (modified after Forte & Bailey, 2007); b) Relationship between kinematic vorticity number W_k and the percentage of pure shear (PS) and simple shear (SS) (modified after Law et al., 2004). The obtained range is indicated; c) relationship between the orientation of the maximum instantaneous stretching axis (ISA max) with respect to the shear zone boundary (angle θ) versus the W_k number (modified after Fossen & Tikoff, 1993). Samples fall in the field of pure shear dominated transpression.

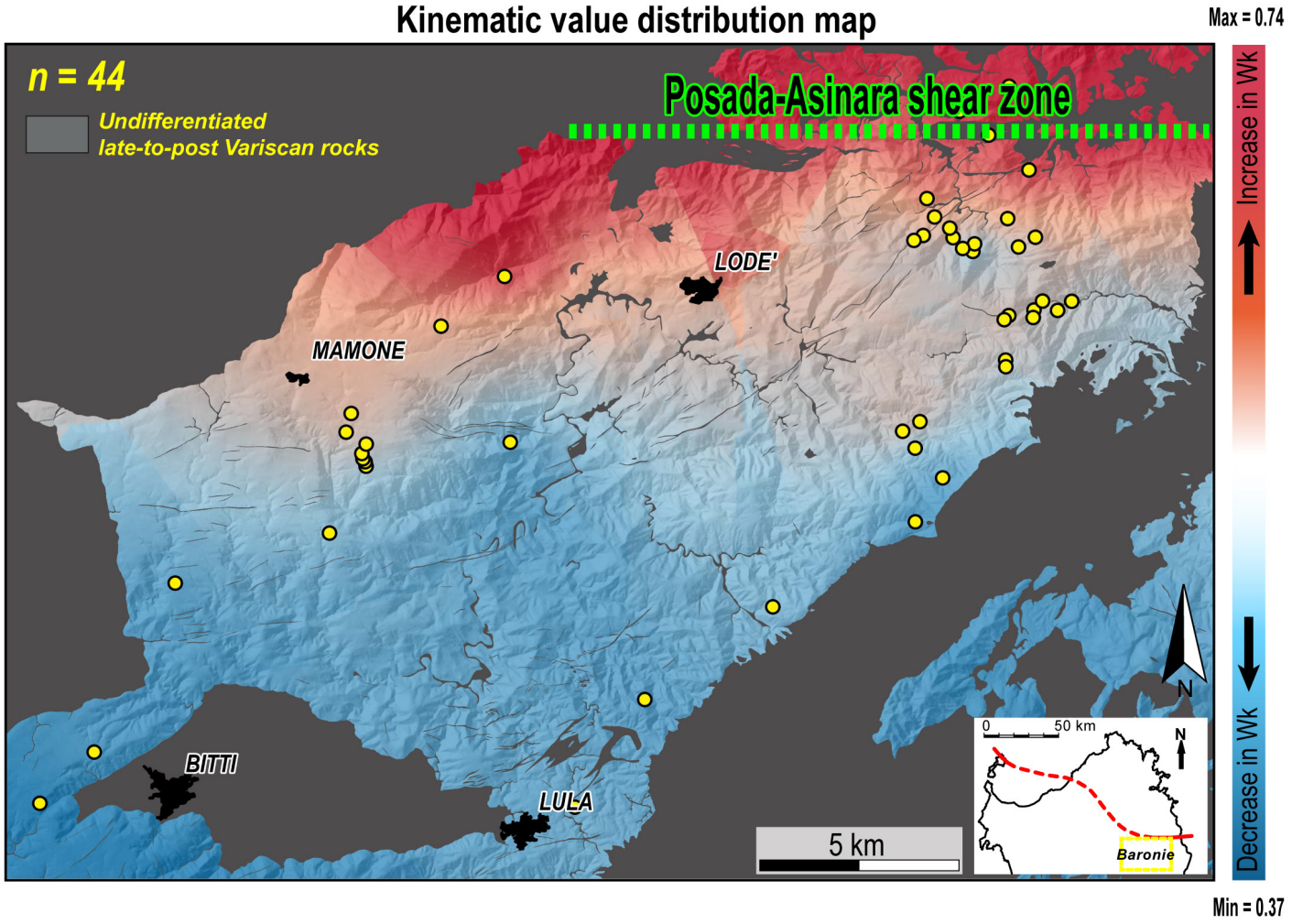

Fig. 5 - W_k contour map of the Baronie region (the contoured area has been highlighted with a yellow square in the northern Sardinia island representation. The position of both the samples investigated in this work and those used by Petroccia (2018) and Carosi et al. (2020) has been displayed with yellow dots.

micro-folds, in microlithons or as an internal foliation in garnet and plagioclase minerals. Although garnet and plagioclase mainly grew between the collisional (D_1) and the transpressional (D_2) event, part of the growth is syn-kinematic with the D_2 shearing. Kinematic indicators point to a top-to-the NW sense of shear, in agreement with Carosi & Palmeri (2002). The PASZ activity is confirmed to be related to the D_2 phase (Carosi et al., 2020), and the syn-kinematic mineral assemblage (biotite + white mica) parallel to the S_2 mylonitic foliation, coupled with the occurrence of GBM (T > 500 °C; Law, 2014) is indicative of amphibolite-facies conditions. However, the syn-kinematic growth of chlorite, both in strain shadows and along the C' planes, is consistent with a metamorphic retrogression towards greenschist-facies during the evolution of the late D_2 phase (Graziani et al., 2020). Furthermore, local incipient SGR, overprinting GBM in quartz, has been recognized, supporting a decrease in the temperature down to the greenschist-facies condition, as also noted by Graziani et al. (2020). In the L–MGMC, our data agree that the shearing event started to be active close to the metamorphic 'peak', under amphibolite-facies conditions (D_2), and lasted up to greenschist-facies conditions during the late D_2 event (Graziani et al., 2020). The transpressive tectonics related to the PASZ continued during the D_3 phase under even shallower crustal conditions (Carosi et al., 2020; Graziani et al., 2020).

The kinematic of the flow allowed us to characterize the deformation in terms of the percentage of pure and simple shear components linked to the PASZ activity in its southernmost sector in the Baronie region. The kinematic vorticity data obtained by the C' shear band method (Kurz & Northrup, 2008) highlighted 75-68% pure shear and 25-32% simple shear components associated with a pure shear dominated transpression. This agrees with the observed progressive increase in the W_k value and in the simple shear component northward, i.e., toward the PASZ high-strain zone (Carosi et al., 2020).

Contour maps are a fundamental tool for analyzing and elaborating spatial geological data. They display the variation of geological variables, such as thickness, depth, or porosity, over an area of interest (Groshong, 2006). Before the advent of fast computers and computational algorithms, maps showing geological variation were prepared by hand. However, hand-contoured maps cannot be reproduced precisely, and values implied by the contours cannot be recovered. Data interpolation in geology is often difficult due to the lack of closely or homogeneously distributed data,

resulting in interpolations conducted with an irregular sampling distribution. As recommended by previous authors (e.g., Fiannacca et al., 2017) and as used in this work, stochastic interpolators depend on the computation of a probability model, which is a mathematical representation of a random phenomenon necessary for these purposes. It is important to recognize that all contouring methods, mathematical or otherwise, are interpolation methods and therefore include an error in the resultant surface. This error is related to both the density and location of the measured control points used to construct the surface. Nevertheless, the amount of W_k estimations linked to the PASZ activity in the Baronie area in Sardinia, integrating both the existing and the new data, is sufficient in number (44 data) to develop a detailed kinematic of the flow contour map (Fig. 5). It is important to note that all the kinematic vorticity data have been derived with the same methods, i.e., the *C'* shear band, but from different lithotypes. In fact, the investigated area by Carosi et al. (2020) is characterized by micaschist and paragneiss from the garnet to the sillimanite + white mica zones and granodioritic and granitic augen orthogneiss and amphibolite lenses within the kyanite-bearing micaschist (Cruciani et al., 2013, 2022, Scodina et al., 2021). Despite most of the investigated lithotypes are associated with similar rheological behaviour due to the presence of a similar rock matrix made by white mica and biotite, a detailed rheological characterization of the present lithotypes is out from the aim of this work. The obtained contour map showing the spatial W_k distribution linked to the PASZ in the Baronie region (Fig. 5), graphically shows a southward increase in the pure shear component, associated with a systematic and progressive northward increase of the simple shear component, from 25% to 52%, in agreement with the Carosi et al. (2020) results. The recognized W_k distribution is not entirely systematic and linear, but few complex zones are detectable (i.e., low W_k values in the Lodè town eastern sector; Fig. 5). The presence of anomalous W_k sectors could be related to: (i) the occurrence of lithotypes with different rheological properties (i.e., orthogneiss and metasedimentary rocks), resulting in a variation of the W_k estimations linked to the different recording of the deformation; (ii) a strain partitioning along the mylonitic belt, giving rise to high- and low-strain zones, or (iii) the uncertainties and contour variation related to the lack of measurements in a specific sector of the investigated area.

Since vorticity analysis is a powerful tool and the kinematics of flow is a fundamental parameter for investigating the complex evolution of regional-scale shear zones, when an adequate amount of estimations is available, graphical-based data like contour and interpolated maps help and improve the traditional data interpretation. In this way, it is possible to explore the W_k distribution, compare the different deformation regimes linked to high- and low-strain domains, identify a possible spatial strain partitioning, unravel the compatibility between strain and structures and develop robust correlations at the belt scale. In addition, despite this approach to represent the flow kinematics being few applied and relatively new, several improvements could be reached by testing it with different scales of observations and in different shear zone types. Thus, as a final remark, I strongly suggest that geospatial investigations about flow kinematics in a collisional framework can be strictly associated with field investigations to unravel the distribution and partitioning of deformation throughout different crustal-scales shear zones.

ACKNOWLEDGEMENTS

I wish to acknowledge my supervisors Rodolfo Carosi, Chiara Montomoli and Salvatore Iaccarino for always giving me great support and many opportunities during the Master and PhD projects. Matteo Simonetti is thanked for his help during my Master Thesis. Jacob Forshaw is thanked for his helpful suggestions. I want to thank Gaetano Ortolano and Chiara Montemagni for their careful suggestions that strongly improved the original manuscript. I also thank the editor, Gianluca Vignaroli, for his careful editorial work and final suggestions.

REFERENCES

Arthaud F. & Matte P. (1977) - Late Paleozoic strikeslip faulting in southern Europe and northern Africa; result of a right-lateral shear zone between the Appalachians and the Urals. Geol. Soc. Am. Bull., 88, 1305-1320, https://doi.org/10.1130/0016-7606(1977)88%3C1305:LPSFIS%3E2.0.CO;2.

Bühler M., Zurbriggen R., Berger A., Herweg M. & Rubatto D. (2022) - Late Carboniferous Schlingen in the Gotthard nappe (Central Alps) and their relation to the Variscan evolution. Int. J. Earth Sci, https://doi.org/10.1007/s00531-022-02247-5.

Bajolet F., Chardon D., Martinod J., Gapais D. & Kermarrec J.J. (2015) - Synconvergence flow inside and at the margin of orogenic plateaus: Lithospheric-scale experimental approach. J. Geophys. Res. Solid Earth, 120(9), 6634-6657, https://doi.org/10.1002/2015JB012110.

Bajolet F., Replumaz A. & Lainé R. (2013) - Orocline and syntaxes formation during subduction and collision. Tectonics, 32(5), 1529-1546, https://doi.org/10.1002/tect.20087.

Boissonnat J.D. & Gazais F. (2002) - Smooth surface reconstruction via natural neighbour interpolation of distance functions. Comput. Geom. Theory Appl. 22 (1-3), 185-203.

Cagnard F., Durrieu N., Gapais D., Brun J.P. & Ehlers C. (2006) - Crustal thickening and lateral flow during compression of hot lithospheres, with particular reference to Precambrian times. Terra Nova, 18(1), 72-78, https://doi.org/10.1111/j.1365-3121.2005.00665.x.

Carmignani L., Carosi R., Di Pisa A., Gattiglio M., Musumeci G., Oggiano G. & Pertusati P.C. (1994) - The hercynian chain in Sardinia (Italy). Geodin. Acta, 7(1), 31-47, https://doi.org/10.1080/09853111.1994.11105257.

Carmignani L., Oggiano G., Barca S., Conti P., Eltrudis A., Funedda A., Pasci S. & Salvadori I. (2001) - Geologia della Sardegna (Note illustrative della Carta Geologica della Sardegna in scala 1:200.000). Memorie descrittive della Carta Geologica d'Italia, Servizio Geologico Nazionale, Istituto Poligrafico e Zecca dello Stato, Roma.

Carosi R. & Malfatti G. (1995) - Analisi Strutturale dell'Unità di Meana Sardo e caratteri della deformazione duttile nel Sarcidano-Barbagia di Seulo (Sardegna centrale, Italia). Atti della Società Toscana di Scienze Naturali, Serie A, 102, 121-136.

Carosi R. & Oggiano G. (2002) - Transpressional deformation in northwestern Sardinia (Italy): insights on the tectonic evolution of the Variscan belt. C. R. - Geosci., 334(4), 287-294, https://doi.org/10.1016/S1631-0713(02)01740-6.

Carosi R. & Palmeri R. (2002) - Orogen-parallel tectonic transport in the Variscan belt of northeastern Sardinia (Italy): implications for the exhumation of medium-pressure metamorphic rocks. Geol. Mag., 139, https://doi.org/10.1017/S0016756802006763.

Carosi R. & Pertusati P.C. (1990) - Evoluzione strutturale delle unità tettoniche erciniche nella Sardegna centro-meridionale. Boll. Soc. Geol. It., 109, 325-335.

Carosi R., D'Addario E., Mammoliti E., Montomoli C. & Simonetti M. (2016) - Geology of the northwestern portion of the Ferriere-Mollieres Shear Zone, Argentera Massif, Italy. J. Maps, 12, 466-475, https://doi.org/10.1080/17445647.2016.1243491.

Carosi R., Di Pisa A., Iacopini D., Montomoli C. & Oggiano G. (2004) - The structural evolution of the Asinara Island (NW Sardinia, Italy). Geodin. Acta, 17, 309-329, https://doi.org/10.3166/ga.17.309-329.

Carosi R., Frassi C., Iacopini D. & Montomoli C. (2005) - Post-collisional transpressive tectonic in northern Sardinia (Italy). J. Virtual Explor., 19, https://doi.org/10.3809/jvirtex.2005.00118.

Carosi R., Montomoli C., Iaccarino S., Benetti B., Petroccia A. & Simonetti M. (2022) - Constraining the timing of evolution of shear zones in two collisional orogens: fusing structural geology and geochronology. Geosciences, 12, 231, https://doi.org/10.3390/geosciences12060231.

Carosi R., Montomoli C., Rubatto D. & Visonà D. (2006) - Normal-sense shear zones in the core of the Higher Himalayan Crystallines (Bhutan Himalaya): Evidence for extrusion?. Geol. Soc. Spec. Publ., 268(1), 425-444.

Carosi R., Petroccia A., Iaccarino S., Simonetti M., Langone A. & Montomoli C. (2020) - Kinematics and timing constraints in a transpressive tectonic regime: the example of the Posada-Asinara shear zone (NE Sardinia, Italy). Geosciences, 10(8), 288, https://doi.org/10.3390/geosciences10080288.

Carosi R., Frassi C. & Montomoli C. (2009) - Deformation during exhumation of medium- and high-grade metamorphic rocks in the Variscan chain in northern Sardinia (Italy). Geol. J., 44, 280-305, https://doi.org/10.1002/gj.1137.

Carosi R., Montomoli C., Tiepolo M. & Frassi C. (2012) - Geochronological constraints on post-collisional shear zones in the Variscides of Sardinia (Italy): Post-collisional shear zones in the Variscides of Sardinia. Terra Nova, 24, 42-51, https://doi.org/10.1111/j.1365-3121.2011.01035.x.

Carreras J. & Druguet E. (2014) - Framing the tectonic regime of the NE Iberian Variscan segment. Geological Society of London, Special Publications, 405, 249-264, https://doi.org/10.1144/SP405.7.

Casini L. & Oggiano G. (2008) - Late orogenic collapse and thermal doming in the northern Gondwana margin incorporated in the Variscan Chain: A case study from the Ozieri Metamorphic Complex, northern Sardinia, Italy. Gondwana Res., 13, 396-406, https://doi.org/10.1016/j.gr.2007.11.004.

Casini L., Funedda A. & Oggiano G. (2010) - A balanced foreland–hinterland deformation model for the Southern Variscan belt of Sardinia, Italy. Geol. J., 45(5-6), 634-649. https://doi.org/10.1002/gj.1208.

Casini L., Maino M., Langone A., Oggiano G., Corvò S., Estrada J. R. & Liesa M. (2023) - HTLP metamorphism and fluid-fluxed melting during multistage anatexis of continental crust (N Sardinia, Italy). J. Metamorph. Geol., 41, 25-27, https://doi.org/10.1111/jmg.12687.

Caso F., Nerone S., Petroccia A. & Bonasera M. (2021) - Geology of the southern Gran Paradiso Massif and Lower Piedmont Zone contact area (middle Ala valley, Western Alps, Italy). J. Maps, 17(2), 237-246, https://doi.org/10.1080/17445647.2021.1911869.

Chardon D., Gapais D. & Cagnard F. (2009) - Flow of ultra-hot orogens: a view from the Precambrian, clues for the Phanerozoic. Tectonophysics, 477(3-4), 105-118, https://doi.org/10.1016/j.tecto.2009.03.008.

Cocco F., Loi A., Funedda A., Casini L., Ghienne J.F., Pillola G.L., Vidal M., Meloni M.A. & Oggiano G. (2022) - Ordovician tectonics of the South European Variscan Realm: new insights from Sardinia. Int. J. Earth Sci., 1-24, https://doi.org/10.1007/s00531-022-02250-w.

Cocco F., Oggiano G., Funedda A., Loi A. & Casini L. (2018) - Stratigraphic, magmatic and structural features of Ordovician tectonics in Sardinia (Italy): a review. J. Iber. Geol., 44, 619-639, https://doi.org/10.1007/s41513-018-0075-1.

Cochelin B., Lemirre B., Denèle Y. & de Saint Blanquat M. (2021) - Strain partitioning within bending orogens, new insights from the Variscan belt (Chiroulet-Lesponne domes, Pyrenees). Tectonics, 40, 386, https://doi.org/10.1029/2020TC006386.

Conand C., Mouthereau F., Ganne J., Lin A.T.S., Lahfid A., Daudet M., Mesalles L., Giletycz S. & Bonzani M. (2020) - Strain partitioning and exhumation in oblique Taiwan collision: Role of rift architecture and plate kinematics. Tectonics, 39(4), e2019TC005798, https://doi.org/10.1029/2019TC005798.

Conti P., Carmignani L., Cerbai N., Eltrudis A., Funedda A. & Oggiano G. (1999) - From thickening to extension in the Variscan belt - kinematic evidence from Sardinia (Italy). Terra Nova, 11(2/3), 93-99, https://doi.org/10.1046/j.1365-3121.1999.00231.x.

Conti P., Carmignani L. & Funedda A. (2001) - Change of nappe transport direction during the Variscan collisional evolution of central-southern Sardinia (Italy). Tectonophysics, 332(1-2), 255-273, https://doi.org/10.1016/S0040-1951(00)00260-2.

Conti P., Funedda A. & Cerbai N. (1998) - Mylonite development in the Hercynian basement of Sardinia (Italy). J. Struct. Geol., 20(2/3), 121-133, https://doi.org/10.1016/S0191-8141(97)00091-6.

Corsini M. & Rolland Y. (2009) - Late evolution of the southern European Variscan belt: Exhumation of the lower crust in a context of oblique convergence. C.R. Geosc., 341, 214-223, https://doi.org/10.1016/j.crte.2008.12.002.

Cruciani G, Franceschelli M., Carosi R. & Montomoli C. (2022) - P-T path from garnet zoning in pelitic schist from NE Sardinia, Italy: Further constraints on the metamorphic and tectonic evolution of the north Sardinia Variscan belt. Lithos, 428-429, https://doi.org/10.1016/j.lithos.2022.106836.

Cruciani G., Franceschelli M., Massonne H.-J., Carosi R. & Montomoli C. (2013) - Pressure–temperature and deformational evolution of high-pressure metapelites from Variscan NE Sardinia, Italy. Lithos, 175-176, 272-284, https://doi.org/10.1016/j.lithos.2013.05.001.

Cruciani G., Montomoli C., Carosi R., Franceschelli M. & Puxeddu M. (2015) - Continental collision from two perspectives: a review of Variscan metamorphism and deformation in northern Sardinia. Periodico di Mineralogia, 84, 657-699, https://doi.org/10.2451/2015PM0455.

Dasgupta S., Mandal N. & Bose S. (2015) - How far does a ductile shear zone permit transpression? In: Mukherjee S., Mulchrone K.F. (Eds), Ductile Shear Zones: From Micro to Macro-scales. Springer, 14-29, https://doi.org/10.1002/9781118844953.ch2.

Dewey J.F., Holdsworth R.E. & Strachan R.A. (1998) - Transpression and Transtension Zones. Geological Society of London, Special Publications, 135(1), 1-14, https://doi.org/10.1144/gsl.sp.1998.135.01.01.

Di Vincenzo G., Carosi R. & Palmeri R. (2004) - The Relationship between Tectono-metamorphic Evolution and Argon Isotope Records in White Mica: Constraints from in situ 40Ar-39Ar Laser Analysis of the Variscan Basement of Sardinia. J. Petrol., 45, 1013-1043, https://doi.org/10.1093/petrology/egh002.

Elter F.M., Musumeci G. & Pertusati P.C. (1990) - Late Hercynian shear zones in Sardinia. Tectonophysics, 176, 387-404. https://doi.org/10.1016/0040-1951(90)90080-R.

Faure M. & Ferrière J. (2022) - Reconstructing the Variscan Terranes in the Alpine Basement: Facts and Arguments for an Alpidic Orocline. Geosciences, 12, 65, https://doi.org/10.3390/geosciences12020065.

Faure M., Rossi P., Gaché J., Melleton J., Frei D., Li X. & Lin W. (2014) - Variscan orogeny in Corsica: new structural and geochronological insights, and its place in the Variscan geodynamic framework. Int. J. Earth Sci., 103, 1533-1551, https://doi.org/10.1007/s00531-014-1031-8.

Fiannacca P., Ortolano G., Pagano M., Visalli R., Cirrincione R. & Zappalà L. (2017) - IG-Mapper: A new ArcGIS® toolbox for the geostatistics-based automated geochemical mapping of igneous rocks. Chem. Geol., 470, 75-92, https://doi.org/10.1016/j.chemgeo.2017.08.024.

Forte A.M. & Bailey C.M. (2007) - Testing the Utility of the Porphyroclast Hyperbolic Distribution Method of Kinematic Vorticity Analysis. J. Struct. Geol., 29(6), 983-1001, https://doi.org/10.1016/j.jsg.2007.01.006.

Fossen H. (2016) - Structural geology, Second edition. ed. Cambridge University Press, Cambridge, United Kingdom, 524 pp.

Fossen H. & Cavalcante G.C.G. (2017) - Shear zones - A review. Earth Sci. Rev., 171, 434-455, https://doi.org/10.1016/j.earscirev.2017.05.002.

Fossen H. & Tikoff B. (1993) - The deformation matrix for simultaneous simple shearing, pure shearing, and volume change, and its application to transpression/transtension tectonics. J. Struct. Geol., 413-422, https://doi.org/10.1016/0191-8141(93)90137-Y.

Fossen H., Tikoff B. & Teyssier C. (1994) - Strain modelling of transpressional and transtensional deformation. Norsk Geol Tidsskr, 74,134-45.

Franceschelli M., Memmi I., Pannuti F. & Ricci C.A. (1989) - Diachronous metamorphic equilibria in the Hercynian basement of northern Sardinia, Italy. Geological Society of London, Special Publications, 43, 371-375, https://doi.org/10.1144/GSL.SP.1989.043.01.33.

Franceschelli M., Memmi I. & Ricci C.A. (1982) - Ca distribution between garnet and plagioclase in pelitic and psammitic schists from the metamorphic basement of north eastern Sardinia. Contrib. Miner. Petr., 80, 285-295, https://doi.org/10.1007/BF00371358.

Franceschelli M., Puxeddu M. & Cruciani G. (2005) - Variscan metamorphism in Sardinia, Italy: review and discussion. J. Virtual Expl., 19, 2, http://dx.doi.org/10.3809%2Fjvirtex.2005.00121.

Franke W., Cocks L.R.M. & Torsvik T.H. (2017) - The Palaeozoic Variscan oceans revisited. Gondwana Res., 48, 257-284, https://doi.org/10.1016/j.gr.2017.03.005.

Frassi C., Carosi R., Montomoli C. & Law R.D. (2009) - Kinematics and vorticity of flow associated with post-collisional oblique transpression in the Variscan Axial Zone of northern Sardinia (Italy). J. Struct. Geol., 31, 1458-1471, https://doi.org/10.1016/j.jsg.2009.10.001.

Frevillé K., Trap P., Melleton J., Vanardois J., Faure M., Bruguier O. & Poujol M. (2022) - Carboniferous tectono-thermal evolution of the Variscan crust in the Belledonne-Pelvoux area. Bull. Société Géologique Fr.

Ghosh P. & Bhattacharyya K. (2022) - Investigating inter-relationships among kinematic vorticity, strain, and minimum translations from shear zones associated with internal thrusts of major fold-thrust belts. Earth Sci. Rev., 231, 104093, https://doi.org/10.1016/j.earscirev.2022.104093.

Giacomini F., Dallai L., Carminati E., Tiepolo M. & Ghezzo C. (2008) - Exhumation of a Variscan orogenic complex: insights into the composite granulitic–amphibolitic metamorphic basement of south-east Corsica (France). J. Metam. Geol., 26, 403-436, https://doi.org/10.1111/j.1525-1314.2008.00768.x.

Gillam B.G., Little T.A., Smith E. & Toy V.G. (2013) - Extensional shear band development on the outer margin of the Alpine mylonite zone, Tatare Stream, Southern Alps, New Zealand. J. Struct. Geol., 54, 1-20, https://doi.org/10.1016/j.jsg.2013.06.010.

Graziani R., Montomoli C., Iaccarino S., Menegon L., Nania L. & Carosi R. (2020) - Structural setting of a transpressive shear zone: Insights from geological mapping, quartz petrofabric and kinematic vorticity analysis in NE Sardinia (Italy). Geol. Mag., 1-19, https://doi.org/10.1017//S0016756820000138.

Groshong R.H. (2006) - 3-D Structural Geology. A Practical Guide to Quantitative Surface and Subsurface Map Interpretation. Springer Berlin, Heidelberg, 400 pp, https://doi.org/10.1007/978-3-540-31055-6.

Harland W.B. (1971) - Tectonic transpression in Caledonian Spitzbergen. Geol. Mag., 108, 27-42, https://doi.org/10.1017/S0016756800050937.

Iacopini D., Carosi R., Montomoli C. & Passchier C.W. (2008) - Strain analysis and vorticity of flow in the northern sardinian variscan belt: Recognition of a partitioned oblique deformation event. Tectonophysics, 446, 77-96, https://doi.org/10.1016/j.tecto.2007.10.002.

Iacopini D., Frassi C., Carosi R. & Montomoli C. (2011) - Biases in three-dimensional vorticity analysis using porphyroclast system: Limits and application to natural examples. Geological Society of London, Special Publications, 360, 301-318, https://doi.org/10.1144/SP360.17.

Law R.D. (2014) - Deformation thermometry based on quartz c-axis fabrics and recrystallization microstructures: A review. J. Struct. Geol., 66, 129-161, https://doi.org/10.1016/j.jsg.2014.05.023.

Law R.D., Searle M.P. & Simpson R.L. (2004) - Strain, deformation temperatures and vorticity of flow at the top of the Greater Himalayan Slab, Everest Massif, Tibet. Journal of the Geological Society, London, 161, 305-320, https://doi.org/10.1144/0016-764903-047.

Jessup M.J., Law R.J. & Frassi C. (2007) - The Rigid Grain Net (RGN): An alternative method for estimating mean kinematic vorticity number (Wm). J. Struct. Geol., 29, 411-421, https://doi.org/10.1016/j.jsg.2006.11.003.

Johnston S.T., Weil A.B. & Gutiérrez-Alonso G. (2013) - Oroclines: Thick and thin. Bulletin, 125(5-6), 643-663, https://doi.org/10.1130/B30765.1.

Jones R.R., Holdsworth R.E., Clegg P., McCaffrey K. & Tavarnelli E. (2004) - Inclined Transpression. J. Struct. Geol., 26(8), 1531-1548, https://doi.org/10.1016/j.jsg.2004.01.004.

Krýza O., Závada P. & Lexa O. (2019) - Advanced strain and mass transfer analysis in crustal-scale oroclinal buckling and detachment folding analogue models. Tectonophysics, 764, 88-109, https://doi.org/10.1016/j.tecto.2019.05.001.

Kurz G.A. & Northrup C.J. (2008) - Structural analysis of mylonitic rocks in the Cougar Creek Complex, Oregon-Idaho using the porphyroclast hyperbolic distribution method, and potential use of SC′-type extensional shear bands as quantitative vorticity indicators. J. Struct. Geol., 30, 1005-1012, https://doi.org/10.1016/j. jsg.2008.04.003.

Massonne H.J., Franceschelli M. & Cruciani G. (2013) - Geothermobarometry on anatectic melts – A high pressure Variscan migmatite from Northeast Sardinia. Int. Geol. Rev., 55, 1490-1505, https://doi.org/10.1080/00206814.2013.78072.

Matte P. (2001) - The Variscan collage and orogeny (480–290 Ma) and the tectonic definition of the Armorica microplate: a review. Terra Nova 13, 122-128, https://doi.org/10.1046/j.1365-3121.2001.00327.x.

Matte P. (1986) - La Chaîne varisque parmi les chaînes paléozoïques péri-atlantiques, modèle d'évolution et position des grands blocs continentaux au Permo-Carbonifère. Bulletin de La Société Géologique de France, 8, 4-24, https://doi.org/10.2113/gssgfbull.II.1.9.

Montemagni C., Carosi R., Fusi N., Iaccarino S., Montomoli C., Villa I. M. & Zanchetta S. (2020) - Three-dimensional vorticity and time-constrained evolution of the Main Central Thrust zone, Garhwal Himalaya (NW India). Terra Nova, 32(3), 215-224, https://doi.org/10.1111/ter.12450.

Montemagni C. & Zanchetta S. (2022) - Constraining kinematic and temporal evolution of a normal-sense shear zone: Insights into the Simplon Shear Zone (Western Alps). Journal of Structural Geology, 156, 104557 https://doi.org/10.1016/j.jsg.2022.104557.

Montomoli C. (2003) - Zone di taglio fragili-duttili nel basamento varisico metamorfico di basso grado della Nurra meridionale (Sardegna nord-occidentale). Atti della Società Toscana di Scienze Naturali, Serie A, 108, 23-29.

Montomoli C., Iaccarino S., Carosi R., Langone A. & Visonà D. (2013) - Tectonometamorphic discontinuities within the Greater Himalayan Sequence in Western Nepal (Central Himalaya): insights on the exhumation of crystalline rocks. Tectonophysics, 608, 1349-1370, https://doi.org/10.1016/j.tecto.2013.06.006.

Montomoli C., Iaccarino S., Simonetti M., Lezzerini M. & Carosi R. (2018) - Structural setting, kinematics and metamorphism in a km-scale shear zone in the inner nappes of Sardinia (Italy). Ital. J. Geosci., 137, 294-310, https://doi.org/10.3301/IJG.2018.16.

Nabavi S.T., Alavi S.A., Díaz-Azpiroz M., Mohammadi S., Ghassemi M.R., Fernàndez C., Barcos L. & Frehner M. (2020) - Deformation Mechanics in Inclined, Brittle-Ductile Transpression Zones: Insights from 3D Finite Element Modelling. J. Struct. Geol., 137, 104082, https://doi.org/10.1016/j.jsg.2020.104082.

Nabavi S.T., Alav S.A., Mohammadi S., Ghassemi M.R. & Frehner M. (2017) - Analysis of Transpression within Contractional Fault Steps Using Finite-Element Method. J. Struct. Geol., 96, 1-20, https://doi.org/10.1016/j.jsg.2017.01.004.

Nania L., Montomoli C., Iaccarino S., Leiss B. & Carosi R. (2022) - Multi-stage evolution of the South Tibetan Detachment System in central Himalaya: Insights from carbonate-bearing rocks. J. Struct. Geol., 158, 104574, https://doi.org/10.1016/j.jsg.2022.104574.

Oberto M. & Petroccia A. (2021) - Preliminary data of the Cannero Riviera mineralized system (Southern Alpine Domain, Western Alps, Italy). Rend. Online Soc. Geol. It., 53, 14-20. http://doi.org/103301/ROL.2021.01.

Ortolano G., Fazio E., Visalli R., Alsop G.I., Pagano M. & Cirrincione R. (2020) - Quantitative microstructural analysis of mylonites formed during Alpine tectonics in the western Mediterranean realm. J. Struct. Geol., 131, 103956, https://doi.org/10.1016/j.jsg.2019.103956.

Ortolano G., Pagano M., Visalli R., Angì G., D'Agostino A., Muto F., Tripodi V., Critelli S. & Cirrincione R. (2022) - Geology and structure of the Serre Massif upper crust: a look in to the late-Variscan strike–slip kinematics of the Southern European Variscan chain. J. Maps, https://doi.org/10.1080/17445647.2022.2057876.

Padovano M., Dörr W., Elter F.M. & Gerdes A. (2014) - The East Variscan Shear Zone: Geochronological constraints from the Capo Ferro area (NE Sardinia, Italy). Lithos, 196-197, 27-41, https://doi.org/10.1016/j.lithos.2014.01.015.

Padovano M., Elter F.M., Pandeli E. & Franceschelli M. (2012) - The East Variscan Shear Zone: new insights into its role in the Late Carboniferous collision in southern Europe. Int. Geol. Rev., 54, 957-970, https://doi.org/10.1080/00206814.2011.626120.

Parui C., Bhattacharyya K. & Ghosh P. (2022) - Penetrative strain and partitioning of convergence-related shallow crustal shortening, across scales, in the Lesser-and Sub-Himalayan thrusts: Insights from the eastern Himalaya, Sikkim. Tectonics, e2022TC007210, https://doi.org/10.1029/2022TC007210.

Passchier C.W. (1987) - Stable positions of rigid objects in non-coaxial flow—a study in vorticity analysis. J. Struct. Geol., 9, 679-690, https://doi.org/10.1016/0191-8141(87)90152-0.

Passchier C.W. & Trouw R.A.J. (2005) - Microtectonics. Springer, Berlin, Heidelberg, https://doi.org/10.1007/3-540-29359-0.

Petroccia A. (2018) - Studio geologico-strutturale e geocronologico di due settori della East Variscan Shear Zone: la Linea Posada-Asinara (Sardegna, Italia) e la Cavalaire Fault (Maures Massif, Francia). Master Thesis, Supervisor Rodolfo C., Co-supervisor Simonetti M., Università degli Studi di Torino, Torino.

Petroccia A., Carosi R., Montomoli C. Iaccarino S. & Vitale Brovarone A. (2022a) - Deformation and temperature variation along thrust-sense shear zones in the hinterland-foreland transition zone of collisional settings: a case study from the Barbagia Thrust (Sardinia, Italy). J. Struct. Geol., 161, https://doi.org/10.1016/j.jsg.2022.104640.

Petroccia A., Carosi R., Montomoli C., Iaccarino S. & Vitale Brovarone A. (2022c) - Thermal variation across collisional orogens: insights from the hinterland-foreland transition zone of the Sardinian Variscan belt. Terra Nova, https://doi.org/10.1111/ter.12635.

Petroccia A., Montomoli C. Iaccarino S. & Carosi R. (2022b) - Geology of the contact area between the Internal and External Nappe Zone of the Sardinian Variscan Belt (Italy): new insights on the complex polyphase deformation occurring in the hinterland-foreland transition zone of collisional belts. J. Maps, https://doi.org/10.1080/17445647.2022.2093660.

Ring U., Bernet M. & Tulloch A. (2015) - Kinematic, finite strain and vorticity analysis of the Sisters shear zone, Stewart Island, New Zealand. J. Struct. Geol., 73, 114-129, https://doi.org/10.1016/j.jsg.2015.02.004.

Sanderson D.J. & Marchini W.R.D. (1984) - Transpression. J. Struct. Geol., 6, 449-458, https://doi.org/10.1016/0191-8141(84)90058-0.

Sarkarinejad K. & Azizi A. (2008) - Slip partitioning and inclined dextral transpression along the Zagros Thrust System, Iran. J. Struct. Geol., 30, 116-136, https://doi.org/10.1016/j.jsg.2007.10.001.

Sarkarinejad K. & Heibati Z. (2017) - Vorticity analysis in the Zagros orogen, Shiraz area, Iran. Int. J. Earth Sci., 106, 2041-2065, https://doi.org/10.1007/s00531-016-1411-3.

Schneider J., Corsini M., Reverso-Peila A. & Lardeaux J.-M. (2014) - Thermal and mechanical evolution of an orogenic wedge during Variscan collision: an example in the Maures-Tanneron Massif (SE France). Geol. Soc. Spec. Publ., 405, 313-331, https://doi.org/10.1144/SP405.4.

Scodina M., Cruciani G. & Franceschelli M. (2021) - Metamorphic evolution and P-T path of the Posada Valley amphibolites: new insights on the Variscan high pressure metamorphism in NE Sardinia, Italy. C. R. - Geosci., 353(1), 227-246.

Simonetti M. (2021) - The East Variscan Shear Zone: a structural and geochronological review for improving paleogeographic reconstruction of the southern Variscides. Rend. Online Soc. Geol. It., 55, 36-52, https://doi.org/10.3301/ROL.2021.13.

Simonetti M. (2022) - A field guide to the excursion in the Maures Massif (southern France): a complete transect of the Southern European Variscan belt. Geol. F. Trips Maps, 14(2.1), 41 pp, https://doi.org/10.3301/GFT.2022.04.

Simonetti M., Carosi R., Montomoli C., Langone A., D'Addario E. & Mammoliti E. (2018) - Kinematic and geochronological constraints on shear deformation in the Ferriere-Mollières shear zone (Argentera-Mercantour Massif, Western Alps): implications for the evolution of the Southern European Variscan Belt. Int. J. Earth Sci., 107, 6, 2163-2189, https://doi.org/10.1007/s00531-018-1593-y.

Simonetti M., Carosi R., Montomoli C., Law R.D. & Cottle J.M. (2021) - Unravelling the development of regional-scale shear zones by a multidisciplinary approach: The case study of the Ferriere-Mollìeres Shear Zone (Argentera Massif, Western Alps). J. Struct. Geol., 149, 104399, https://doi.org/10.1016/j.jsg.2021.104399.

Simonetti M., Carosi R., Montomoli C., Cottle J.M. & Law R.D. (2020a) - Transpressive Deformation in the Southern European Variscan Belt: New Insights from the Aiguilles Rouges Massif (Western Alps). Tectonics, 39, https://doi.org/10.1029/2020TC006153.

Simonetti M., Carosi R., Montomoli C., Corsini M., Petroccia A., Cottle J.M. & Iaccarino S. (2020b) - Timing and kinematics of flow in a transpressive dextral shear zone, Maures Massif (Southern France). Int. J. Earth Sci., 109, 2261-2285, https://doi.org/10.1007/s00531-020-01898-6.

Simpson C. & De Paor D.G. (1993) - Strain and kinematic analysis in general shear zones. J. Struct. Geol., 15(1), 1-20.

Stipp M., Stünitz H., Heilbronner R. & Schmid S.M. (2002) - Dynamic recrystallization of quartz: correlation between natural and experimental conditions. Geological Society of London, Special Publications, 200, 171-190, https://doi.org/10.1144/GSL.SP.2001.200.01.11.

Sullivan W.A. & Law R.D. (2007) - Deformation path partitioning within the transpressional White Mountain shear zone, California and Nevada. J. Struct. Geol., 29, 583-598, https://doi.org/10.1016/j.jsg.2006.11.001.

Teyssier C. & Whitney D.L. (2002) - Gneiss domes and orogeny. Geology, 30(12), 1139-1142, https://doi.org/10.1130/0091-7613(2002)030%3C1139:GDAO%3E2.0.CO;2.

Teyssier C., Tikoff B. & Markley M. (1995) - Oblique plate motion and continental tectonics. Geology, 23, 447-450, https://doi.org/10.1130/0091-7613(1995)023%3C0447:OPMACT%3E2.3.CO;2.

Thigpen J.R., Law R.D., Lloyd G.E., Brown S.J. & Cook B. (2010) - Deformation temperatures, vorticity of flow and strain symmetry in the Loch Eriboll mylonites, NW Scotland: implications for the kinematic and structural evolution of the northernmost Moine Thrust zone. Geological Society of London, Special Publications, 335, 623-662, https://doi.org/10.1144/sp335.26.

Tikoff B. & Fossen H. (1993) - Simultaneous pure and simple shear: the unifying deformation matrix. Tectonophysics, 217, 267–283, https://doi.org/10.1016/0040-1951(93)90010-H.

Tikoff B. & Fossen H. (1995) - The Limitations of Three-Dimensional Kinematic Vorticity Analysis. J. Struct. Geol., 17(12), 1771-1784, https://doi.org/10.1016/0191-8141(95)00069-p.

Torvela T. & Kurhila M. (2020) - How does orogenic crust deform? Evidence of crustal-scale competent behaviour within the partially molten middle crust during orogenic compression. Precambrian Res., 342, 105670. https://doi.org/10.1016/j.precamres.2020.105670.

Vanardois J., Trap P., Roger F., Melleton J., Marquer D., Paquette J.L., Goncalves P., Cagnard F. & Le Bayon B. (2022) - Deformation, crustal melting and magmatism in the crustal-scale East-Variscan Shear Zone (Aiguilles-Rouges and Mont-Blanc massifs, Western Alps). J. Struct. Geol., 163, https://doi.org/10.1016/j.jsg.2022.104724.

Von Raumer J. & Bussy F. (2004) - Mont Blanc and Aiguilles Rouges geology of their polimetamorphic basement. Mémoires de Géologie. Lausanne.

Warr L.N. (2021) - IMA–CNMNC approved mineral symbols. Mineral. Mag., 85, 291-320, https://doi.org/10.1180/mgm.2021.43.

Xypolias P. (2010) - Vorticity analysis in shear zones: A review of methods and applications. J. Struct. Geol., 32, 2072-2092, https://doi.org/10.1016/j.jsg.2010.08.009.

Xypolias P. & Kokkalas S. (2006) - Heterogeneous Ductile Deformation along a Mid-Crustal Extruding Shear Zone: An Example from the External Hellenides (Greece). Geological Society, London, Special Publications, 268(1), 497-516, https://doi.org/10.1144/gsl.sp.2006.268.01.23.